



Dielectric and photovoltaic phenomena in tungsten-doped $\text{Pb}(\text{Mg}_{1/3}\text{Nb}_{2/3})_{1-x}\text{Ti}_x\text{O}_3$ crystal

Chi-Shun Tu, F.-T. Wang, R. R. Chien, V. Hugo Schmidt, C.-M. Hung, and C.-T. Tseng

Citation: *Applied Physics Letters* **88**, 032902 (2006); doi: 10.1063/1.2165278

View online: <http://dx.doi.org/10.1063/1.2165278>

View Table of Contents: <http://scitation.aip.org/content/aip/journal/apl/88/3?ver=pdfcov>

Published by the [AIP Publishing](#)

Articles you may be interested in

[Dielectric/piezoelectric resonance in high-strain \$\text{Pb}\(\text{Mg}_{1/3}\text{Nb}_{2/3}\)_{1-x}\text{Ti}_x\text{O}_3\$ crystals](#)

J. Appl. Phys. **97**, 126105 (2005); 10.1063/1.1948523

[Effect of anisotropic in-plane strains on phase states and dielectric properties of epitaxial ferroelectric thin films](#)

Appl. Phys. Lett. **86**, 052903 (2005); 10.1063/1.1855389

[Growth and characterization of Fe-doped \$\text{Pb}\(\text{Zn}_{1/3}\text{Nb}_{2/3}\)\text{O}_3 - \text{PbTiO}_3\$ single crystals](#)

J. Appl. Phys. **93**, 9257 (2003); 10.1063/1.1571966

[Low-temperature transverse dielectric and pyroelectric anomalies of uniaxial tungsten bronze crystals](#)

J. Appl. Phys. **92**, 1536 (2002); 10.1063/1.1491995

[Pseudolinearity in the inverse dielectric susceptibility of poled \$\text{Pb}\(\text{Mg}_{1/3}\text{Nb}_{2/3}\)\text{O}_3 - \text{PbTiO}_3\$ crystals](#)

J. Appl. Phys. **92**, 638 (2002); 10.1063/1.1483111

The image shows the cover of an Applied Physics Reviews journal. It features a blue and orange color scheme with a molecular structure in the background. The text 'NEW Special Topic Sections' is prominently displayed in white. Below it, 'NOW ONLINE' is written in yellow, followed by the title 'Lithium Niobate Properties and Applications: Reviews of Emerging Trends' in white. The AIP Applied Physics Reviews logo is in the bottom right corner.

NEW Special Topic Sections

NOW ONLINE
Lithium Niobate Properties and Applications:
Reviews of Emerging Trends

AIP Applied Physics
Reviews

Dielectric and photovoltaic phenomena in tungsten-doped $\text{Pb}(\text{Mg}_{1/3}\text{Nb}_{2/3})_{1-x}\text{Ti}_x\text{O}_3$ crystal

Chi-Shun Tu^{a)} and F.-T. Wang*Graduate Institute of Applied Science and Engineering, Fu Jen University, Taipei 242, Taiwan*

R. R. Chien and V. Hugo Schmidt

Department of Physics, Montana State University, Bozeman, Montana 59717

C.-M. Hung and C.-T. Tseng

Department of Physics, Fu Jen University, Taipei 242, Taiwan

(Received 16 September 2005; accepted 13 December 2005; published online 17 January 2006)

This work investigates dielectric and photovoltaic behaviors in $\text{Pb}(\text{Mg}_{1/3}\text{Nb}_{2/3})_{0.64}\text{Ti}_{0.36}\text{O}_3$ single crystal doped with 0.5 mol % WO_3 . Dielectric permittivities measured as functions of temperature and frequency reveal two first-order-type phase transitions upon heating and cooling. The photovoltaic response strongly depends on illumination wavelength, sample thickness, and prior electric-field poling. The relation of photovoltage and light intensity under near-ultraviolet ($\lambda = 406$ nm) illumination for the poled samples can be expressed by an exponential equation. Optical transmission reveals that the cutoff wavelength is near 400 nm and indicates a minimum electronic energy gap of ~ 3.0 eV. © 2006 American Institute of Physics. [DOI: 10.1063/1.2165278]

High-strain ferroelectric $\text{Pb}(\text{Mg}_{1/3}\text{Nb}_{2/3})_{1-x}\text{Ti}_x\text{O}_3$ (PMNT $_x$) single crystals have demonstrated very large piezoelectric coefficients compared with $\text{Pb}(\text{Zr}_{1-x}\text{Ti}_x)\text{O}_3$ ceramics.¹ Physical properties of PMNT strongly depend on Ti content, external electric (E)-field, and crystallographic orientation.¹⁻⁴ The ultrahigh piezoelectricity has been theoretically attributed to polarization rotations between tetragonal (T) and rhombohedral (R) phases through intermediate monoclinic (M) or orthorhombic (O) symmetries.⁵

Photostrictive effect, which directly converts photonic energy to mechanical motion and is originated from the coupling of photovoltaic field and converse piezoelectric response, has the great potential of applications in wireless photoactuators. The tungsten-doped $\text{Pb}_{1-x}\text{La}_x(\text{Zr}_y\text{Ti}_{1-x/4}\text{O}_3)$ ceramics, i.e., PLZT($x/y/z$), exhibits a large photovoltaic effect and photoinduced strain under near-ultraviolet illumination.⁶⁻¹⁰ The photovoltage exhibits obvious dependence on polarization direction of illumination light in PLZT(3/52/48) ceramics doped with WO_3 and Ta_2O_5 .⁷ The optimal illumination wavelength for obtaining maximum photovoltage is 366 nm for PLZT(3/52/48) ceramics. It was found that the photoinduced electric response is sensitive to sample thickness and surface roughness in 0.5 mol % WO_3 -doped PLZT(3/52/48) ceramic and the optimum thickness is 33 μm .⁸⁻¹⁰ The cutoff of optical transmission for PLZT ceramics was observed near 400 nm.¹¹ A recent study showed that the photovoltage of PLZT ceramics depends on grain size and can reach 6 kV/cm with grain size 0.42 μm .¹² The photovoltage across a single grain (in ceramics) is theoretically proportional to the electric polarization along the photovoltaic direction, suggesting that a higher poling field is needed to induce stronger photovoltage.¹³ Impurity doping, which can enhance structural asymmetry and electric conductivity, is believed to play a critical role in the photoinduced electric and elastic phenomena.

Photovoltaic studies to date in ferroelectric materials have mainly focused on the PLZT ceramics. However, the physical origin of photoinduced voltaic response still remains unclear. In this work, we have investigated dielectric and photovoltaic properties in the high-strain PMNT 36% single crystal doped with 0.5 mol % WO_3 , i.e., PMNT/W(36/0.5). The crystal was grown using a modified Bridgman method by H.C. Materials Corp. The samples were cut perpendicular to the $\langle 001 \rangle$ direction and the edges' orientations are $\langle 010 \rangle$ and $\langle 001 \rangle$. The Ti concentration was estimated by using the dielectric maximum temperature T_m .¹⁴ For dielectric measurements, a Wayne-Kerr Precision Analyzer PMA3260A with four-lead connections was used to obtain real (ϵ') and imaginary (ϵ'') parts of dielectric permittivity. A Janis CCS-450 cold head was used with a Lakeshore 340 temperature controller. The sample dimensions are $5 \times 5 \times 1$ mm³ and gold electrodes were deposited on sample surfaces by dc sputtering. Two processes were used in the dielectric measurements, called "zero-field heated" (ZFH) and "zero-field cooled" (ZFC), in which the data were taken upon heating and cooling, respectively, without any E -field poling. The hysteresis loop of polarization versus E field was taken at room temperature (RT) by using a Sawyer-Tower circuit at $f=46$ Hz.

In photovoltaic measurements, argon and krypton ion lasers with wavelengths 488 and 406 nm were used for photonic energies, respectively. The experimental setup is given in Fig. 1. The basal dimensions of samples are 5.0×2.5 mm². The laser polarization is perpendicular to the direction of the prior E -field poling for the poled samples, which were poled at RT. No external dc E field was applied on samples during measurements. Transparent conductive films of indium tin oxide (ITO) were deposited on sample surfaces by sputtering. Note that both ITO film and glass have an optical cutoff near 300 nm. A Thermo Electron EV500 ultraviolet (UV)-Visible Spectrophotometer was used for optical transmission study.

^{a)} Author to whom all correspondence should be addressed; electronic mail: cstu@physics.montana.edu

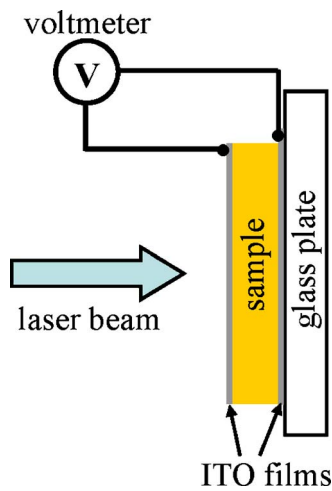


FIG. 1. (Color online) Experimental configuration of photovoltage (V/cm).

Figure 2 shows temperature-dependent ϵ' and ϵ'' at several frequencies obtained from ZFH and ZFC, respectively. Obvious thermal hystereses are observed in the temperature regions of ~ 250 – 310 K and ~ 430 – 450 K respectively, indicating two first-order-type transitions. As shown in the reciprocal of ϵ' [Fig. 2(a)], two steep dips are seen at 316 (291 K) and 444 (439 K), respectively. This also confirms two first-order-type transitions upon heating (cooling). The maximum temperatures (T_m) of ϵ' (ZFH) and ϵ' (ZFC) occur at 444 and 439 K, respectively, where tetragonal (T)-cubic (C) transitions take place. Note that the tungsten trioxide (WO_3) has a monoclinic (M) ferroelectric phase and exhibits high electric conductivity at RT.¹⁵ The phase diagram of PMNT revealed by synchrotron diffraction, predicts a $M \rightarrow T$ transition near RT for PMNT 36%.⁴ Thus, the PMNT/W(36/0.5) crystal likely undergoes a $M \rightarrow T \rightarrow C$ transition sequence near 316 (291 K) and 444 (439 K) upon heating (cooling). In addition, dielectric absorptions ϵ'' (ZFH) and ϵ'' (ZFC) exhibit frequency-dependent maxima

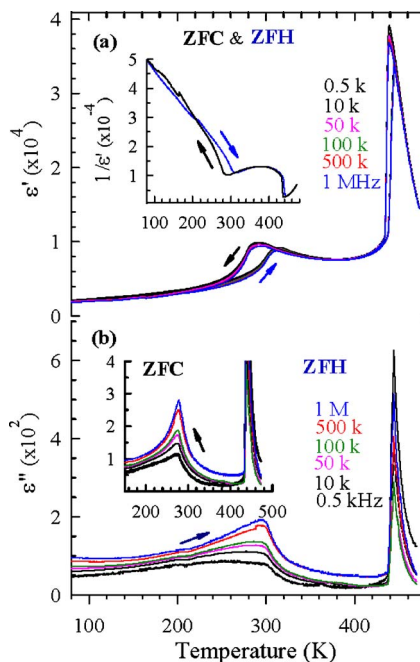


FIG. 2. (Color online) ZFC and ZFH dielectric permittivities of (a) ϵ' and (b) ϵ'' . The inset in (a) is the reciprocal of ϵ' taken from $f=10$ kHz.

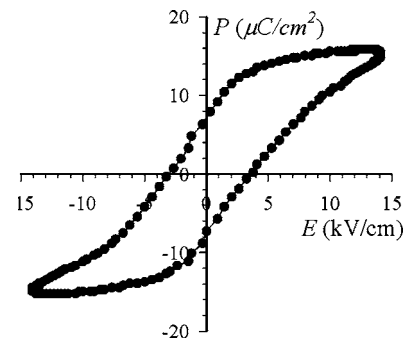


FIG. 3. Hysteresis loop of polarization vs E field obtained at RT.

near 300 and 280 K respectively, but their maximum temperatures are frequency independent. These dielectric behaviors are different from the WO_3 -doped PMNT 33% ceramics.¹⁶

Hysteresis loop of polarization versus E -field taken at RT is given in Fig. 3. The spontaneous polarization and coercive field are about $14 \mu\text{C}/\text{cm}^2$ and $3.5 \text{ kV}/\text{cm}$, respectively. The remnant polarization $\sim 8 \mu\text{C}/\text{cm}^2$ is obviously smaller than $\sim 17 \mu\text{C}/\text{cm}^2$ in PMNT 35% single crystal,¹⁷ likely due to enhancement of electric conductivity by WO_3 dopant.

Figure 4 shows relations of photovoltage and light intensity under blue ($\lambda=488 \text{ nm}$) illumination for thicknesses $d=0.2$ and 0.5 mm . The photovoltaic response strongly depends on sample thickness and the thinner sample has higher photovoltage. Thickness-dependent photovoltaic behavior was also observed in the 0.5 mol% WO_3 -doped PLZT ceramics.^{8–10} Relations of photovoltage and light intensity under illuminations of $\lambda=488$ and 406 nm for $d=0.2 \text{ mm}$ are given in Fig. 5 for unpoled and poled samples. The poled samples with prior polings at $E=5$ and $10 \text{ kV}/\text{cm}$ exhibit similar photovoltaic responses and have much larger photovoltage than the unpoled sample. A prior E -field poling can also enhance the photovoltage in PLZT ceramics due to the increase of remnant polarization.¹² Compared with $\lambda=488 \text{ nm}$, near-UV ($\lambda=406 \text{ nm}$) illumination induces much stronger photovoltaic responses. It indicates that the photonic energy of $\lambda=406 \text{ nm}$ can be absorbed more effectively in the poled sample, because the photovoltage is excited by the photonic absorption. Wavelength-dependent transmission as seen in Fig. 6 confirms that the cutoff occurs at $\sim 400 \text{ nm}$ and indicates a minimum electronic energy gap of $\sim 3.0 \text{ eV}$

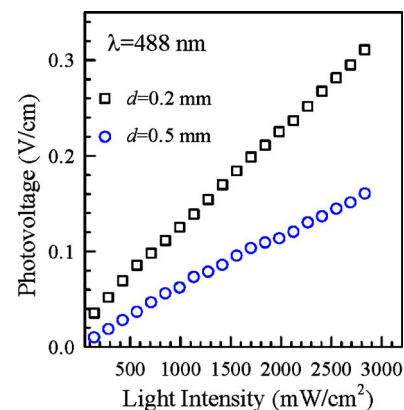


FIG. 4. (Color online) Photovoltage vs light intensity ($\lambda=488 \text{ nm}$) for the unpoled samples.

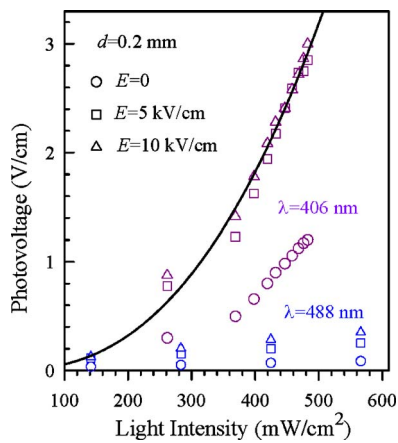


FIG. 5. (Color online) Photovoltage vs light intensity ($\lambda=406$ and 488 nm) for various prior poling E fields. The solid line is the fitting of equation, $E_{ph}=5.7 \times 10^{-7}(I_{op})^{2.5}$, for the poled samples under $\lambda=406$ nm illumination.

($E_g \cong hc/\lambda$). The optical transmission of pure PMNT crystals also goes down to zero at $\lambda \cong 400$ nm.¹⁷

A $T(M)$ and T multidomain phases were observed at RT, respectively, in PMNT 35% and 38% single crystals after a prior poling of $E=6$ kV/cm along $[001]$.³ “ $T(M)$ ” represents that dominant tetragonal domains coexist with a smaller fraction of monoclinic domains. It was found that tetragonal domain increases with Ti content while the sample was poled along $[001]$.³ Thus, the $[001]$ -poled PMNT/W(36/0.5) crystal likely has dominant tetragonal macrodomains at RT.

It was found that the relation of photovoltage and light intensity can be described by an exponential equation. As indicated by the solid line in Fig. 5, the light intensity-

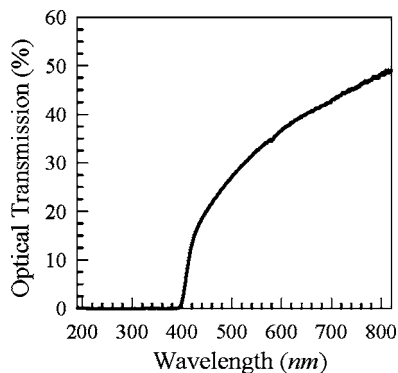


FIG. 6. Optical transmission vs wavelength taken at RT.

dependent photovoltages under near-UV ($\lambda=406$ nm) illumination for the poled samples can be approximately described by $E_{ph}=5.7 \times 10^{-7}(I_{op})^{2.5}$. E_{ph} (V/cm) and I_{op} (mW/cm²) are photovoltage and light intensity, respectively. In poled PLZT(3/52/48) ceramic doped with 0.5 mol % WO_3 , the intensity-dependent photovoltage under illumination of $\lambda=366$ nm can also be described by an exponential equation, $E_{ph}=0.66(I_{op})^{0.5}$.⁹

In conclusion, dielectric and photovoltaic phenomena have been investigated in PMNT/W(36/0.5) single crystal. Two first-order-type phase transitions were observed upon heating and cooling. The photovoltaic response exhibits a strong dependence on illumination wavelength, sample thickness, and E -field poling. The relation of light intensity versus photovoltage under illumination of $\lambda=406$ nm can be expressed by an exponential equation in the poled samples. The optical cutoff at 400 nm suggests that a shorter wavelength may excite stronger photovoltage.

This work was supported by DoE EPSCoR Grant No. DE-FG02-01ER45869 and NSC Grant No. 94-2112-M-030-004.

- ¹T. R. Shrout, Z. P. Chang, N. Kim, and S. Markgraf, *Ferroelectr., Lett. Sect.* **12**, 63 (1990).
- ²Z.-G. Ye, B. Noheda, M. Dong, D. Cox, and G. Shirane, *Phys. Rev. B* **64**, 184114 (2001).
- ³C.-S. Tu, R. R. Chien, F.-T. Wang, and V. H. Schmidt, *Phys. Rev. B* **70**, 220103(R) (2004).
- ⁴B. Noheda, D. E. Cox, G. Shirane, J. Gao, and Z.-G. Ye, *Phys. Rev. B* **66**, 054104 (2002).
- ⁵H. Fu and R. E. Cohen, *Nature (London)* **403**, 281 (2000).
- ⁶K. Uchino, *IEEE Ultrasonics Symposium* (IEEE, New York, 1990), p. 721.
- ⁷S.-Y. Chu, Z. Ye, and K. Uchino, *Smart Mater. Struct.* **3**, 114 (1994).
- ⁸P. Poosanaas, A. Dogan, S. Thakoor, and K. Uchino, *J. Appl. Phys.* **84**, 1508 (1998).
- ⁹P. Poosanaas, K. Tonooka, and K. Uchino, *Mechatronics* **10**, 467 (2000).
- ¹⁰K. Uchino, P. Poosanaas, and K. Tonooka, *Ferroelectrics* **264**, 303 (2001).
- ¹¹M. Ichiki, J. Akedo, Y. Morikawa, K. Ozaki, M. Tanaka, and Y. Ishikawa, *Ferroelectrics* **232**, 259 (1999).
- ¹²K. Takagi, S. Kikuchi, and J.-F. Li, *J. Am. Ceram. Soc.* **87**, 1477 (2004).
- ¹³P. S. Brody and F. Crowne, *J. Electron. Mater.* **4**, 955 (1975).
- ¹⁴Z. Feng, H. Luo, Y. Guo, T. He, and H. Xu, *Solid State Commun.* **126**, 347 (2003).
- ¹⁵F. Jona and G. Shirane, *Ferroelectric Crystals* (Pergamon, New York, 1962), pp. 254, 255.
- ¹⁶N. Zhong, X. L. Dong, D. Z. Sun, P. H. Xiang, and H. Du, *MRS Bull.* **39**, 175 (2004).
- ¹⁷C.-S. Tu, F.-T. Wang, R. R. Chien, V. H. Schmidt, and G. F. Tuthill, *J. Appl. Phys.* **97**, 064112 (2005).